Available online at www.sciencedirect.com

SciVerse ScienceDirect

Ceramics International 38 (2012) 3747–3755

CERAMICS INTERNATIONAL

www.elsevier.com/locate/ceramint

Low loss alumina dielectrics by aqueous tape casting: The influence of composition on the loss tangent

Jozef Chovanec [a,*], Dušan Galusek [a], Jozef Ráheμ [b], Pavol Šajgalík [c]

[a] Vitrum Laugaricio – Joint Glass Centre of the IIC SAS, TnU AD, FChPT STU and RONA, a.s., Študentská 2, SK-911 50 Trenčín, Slovak Republic

[b] Kotlářská 2, 611 37 Brno, Czech Republic

[c] Institute of Inorganic Chemistry, Slovak Academy of Sciences, Dúbravskácesta 9, SK-845 36 Bratislava, Slovak Republic

Received 9 September 2011; received in revised form 9 January 2012; accepted 10 January 2012

Available online 16 January 2012

Abstract

Polycrystalline aluminas with various concentrations of oxide dopants CaO, MgO, and TiO_2, ranging from 0.05 wt.% to 5 wt.% (3 wt.% in case of MgO), as well as pure alumina references were prepared by tape casting of aqueous suspensions and sintered in air at 1600 °C for 4 h for applications as low dielectric loss electroceramics. Loss tangents were measured at room temperature in the frequency range between 1 and 100 kHz as the key parameter for the intended application. The values of loss tangents of doped materials were influenced by the concentration of dopants. The addition of 0.5 and 5 wt.% of TiO_2 and 3 wt.% of MgO decreased the value of loss tangent in the whole frequency range. The addition of these dopants eliminated abnormal grain growth and decreased the amount of residual porosity. By doing so, the dopants compensated the negative influence of process impurities and decreased the loss tangent values. The cations (Ti^{4+}) with high solubility in the Al_2O_3 crystal lattice were preferably built into the grain boundary glass, thus efficiently reducing the concentration of polarizable defects in corundum matrix; the formation of vitreous phase had a positive effect on the value of loss tangent in TiO_2 doped samples. The increased values of loss tangent were related to lower density of prepared materials, and the presence of residual porosity. Other contributing factors were especially the formation of calcium-containing secondary crystalline phases, and the increased concentration of lattice defects due to incorporation of atoms with different valencies to alumina crystal lattice.

Keywords: Tape casting; Loss tangent; Alumina; Dopants

1. Introduction

Among various other applications, alumina-based ceramic sheets are used as the essential part of the diffuse coplanar surface barrier discharge (DCSBD) [1–3] electrode system. This has been with success applied for generation of non-isothermal plasma applicable for mass treatment of materials with low added value, specifically textiles, paper, artificial and natural fibers, glass, wood and metal sheets. In order to enhance the efficiency of non-isothermal plasma generation, dielectric losses in ceramic substrates must be minimized.

The dielectric losses can be divided into two groups: intrinsic and extrinsic. Intrinsic losses depend on crystal structure and express the interaction of crystal lattice with external electric field. Extrinsic losses relate to materials' microstructure, e.g. the presence of microstructural defects, porosity, microcracks and impurities [4]. In high-purity single crystal sapphire the only dielectric loss over a wide frequency range originates from the interaction of electromagnetic fields with crystal lattice vibrations, resulting in very low loss tangents values [5].

In sintered polycrystalline alumina ceramics the presence of impurities or deliberately added dopants can influence the polarizability, and hence the dielectric losses expressed in terms of the loss tangent, of alumina in fundamental way. During sintering the dopants react with alumina, yielding respective aluminates, or diffuse into the alumina crystal lattice creating polarizable point defects. The presence of impurities gives rise to relaxation processes in the MHz frequency region. Important impurities are especially those with a valence different from the

* Corresponding author.
E-mail address: jozef.chovanec@stuba.sk (J. Chovanec).

0272-8842/$36.00
doi:10.1016/j.ceramint.2012.01.020

host (Al^{3+} in our case). The charge imbalance causes the creation of defects in their surroundings for charge compensation, forming an electrical dipole [6–10]. Apart from the valency of metal impurities, their influence on dielectric losses is determined also by their solubility in the host lattice. The solubility of dopants in alumina crystal lattice is usually considered to be very low (in the order of 10–100 ppm) [11], but the published data from various sources vary significantly. Greskovich and Brewer [12] established the solubility of MgO in Al_2O_3 to be 75 ppm at 1720 °C, Roy and Coble [11] reported 300 ppm at 1630 °C, Ando and Momoda [13] 55 ppm at 1700 °C, and Miller et al. [14] 132 ppm at 1600 °C. Winkler et al. established the solubility of TiO_2 to be 500–600 ppm at 1300 °C [15], while McKee and Aleshin measured the solubility of the same metal ion to be 1, 1.8, and 2.5 mol.% at 1400 °C, 1600 °C, and 1700 °C, respectively [16]. The solubility of CaO in Al_2O_3 is estimated to be 30 ppm at 1900 °C in air [17]. Reported values of loss tangent for polycrystalline alumina in the frequency range 1–100 kHz thus typically vary in the order of magnitude from 10^{-4} to 10^{-5} [18,19], but the influence of lattice defects introduced by dopants on dielectric losses has not been conclusively established. The works [18,19] report the values of loss tangent in the interval from 5×10^{-5} to 5×10^{-3} for Al_2O_3 doped with MgO in the frequency range from 10^3 to 10^5 Hz. The effect of Mg addition on the loss tangent of alumina at 20 GHz has been demonstrated by Mollá et al. [19], who reported the increase of $\tan\delta$ from 10^{-4} to 10^{-3} with increasing MgO concentration from 10^{-3}% to 1 wt.%. The samples doped with 0.5 wt.% of TiO_2 showed extremely low values of loss tangent; 2×10^{-5} at 14 GHz [20].

The dopants added in concentrations exceeding their lattice solubility limits may influence the dielectric losses through modification of the ceramics' microstructure. High level of doping results either in atomic segregation of the additives at alumina–alumina grain boundaries, formation of amorphous grain boundary film or, at higher concentrations, in formation of various secondary crystalline phases, such as $MgAl_2O_4$ spinel in case of MgO, various calcium aluminates and Al_2TiO_5 in case of CaO and TiO_2 doping, respectively, with profound influence on final microstructure of the ceramics.

Currently, one of the main methods used for the manufacture of flat ceramic substrates with precisely controlled thickness and consistency is the technique known as tape casting. This method basically starts with specially formulated slurry, which can be cast by a blade to flat sheets or layers. These are dried into flexible solid tapes and sintered into hard ceramic substrate layers [21]. To prepare a slurry with desired flow properties a range of organic processing additives, including binders, dispersants, plastificators, de-foaming agents, etc., often of technical purity, are used. As they represent a substantial part of the ceramic slurry, the amount of impurities introduced by processing aids may be significant, and apart from sinterability and microstructure development they can influence also the dielectric properties of sintered ceramics.

In addition to our previous paper dealing with dielectric losses of model systems with carefully controlled chemical composition [22] this paper is focused at investigation of the influence of combination of dopants on loss tangent of polycrystalline alumina in the frequency range 20–100 kHz. This frequency area has not been studied in detail since most authors focus on dielectric properties in the frequency range characteristic for microwave radiation [4,23,24,18]. Apart from deliberately added metal ions the ceramics studied in this paper contain numerous other impurities originating from organic processing aids used in the process of tape casting. Their influence on loss tangent and on the microstructure parameters of alumina ceramics, such as residual porosity, presence of vitreous or crystalline secondary phases is discussed.

2. Experimental

Polycrystalline alumina samples with various concentrations of oxide dopants CaO, MgO and TiO_2 ranging from 0.05 wt.% to 5 wt.% (3 wt.% for MgO) as well as pure alumina reference materials were prepared by tape casting from suspension with 42.6% of solid (Al_2O_3 powder CT3000 LS SG, Almatis, Germany). Nominal average particle size and specific surface area of the powder are 500 nm and 7.8 $m^2\ g^{-1}$, respectively. Doped specimens were in all cases prepared from the aqueous suspension with 51.2 wt.% of alumina. MgO was added to the suspension in the form of magnesium aluminum spinel $MgAl_2O_4$ (Baikalox S30CR powder, average particle size 190 nm, specific surface area 32 $m^2\ g^{-1}$). TiO_2 was added also in the powder oxide form (extra pure, Riedel de Haen). CaO was added in the form of $CaCO_3$ (extra pure, Lachema, o. p. Brno, Czech Republic). The preparation of a suspension suitable for tape casting process consisted of two major steps. First, stable suspensions were prepared. This was achieved by its electrostatic stabilization by addition of 2 wt.% (with respect to alumina powder) of the dispersant Darvan C-N (R.T. Vanderbilt Company, Inc., aqueous solution of ammonium polymethacrylate – 25 wt.% solution) to suspension of Al_2O_3 powder in water and subsequent 2 h ball milling. In the second step, required plastic properties were achieved by the addition of different organic processing aids. As a binder, Duramax B-1014 (Rohm and Haas Company, aqueous suspension of high molecular weight acryl polymer) was used together with plasticizer PEG 400 (Lambent Technologies Corp.). In order to decrease the surface tension and to de-foam the suspension Dow Corning® DB-310 was added (Dow Corning S. A., Belgium, silicon emulsion). After 2 h of ball milling, the alumina balls were removed by passing the slurry through a plastic sieve. The suspension was then homogenized for 20 h at low speed in order to de-gas the slurry.

The prepared suspension was cast on the device ProCast TC-71 LC (HED International Inc., USA) onto a polymer carrier Mylar (Richard E. Mistler, Inc., USA) with water resistant hydrophobic surface treatment. The parameters of casting were set as follows: the viscosity of suspension between 3.0 and 4.0 Pa s^{-1} at the shear rate 1 s^{-1}, tape thickness 0.7 mm, tape width 90 mm, and shift speed of Mylar tape 7 mm s^{-1}. The green tape was then dried for 24 h at room temperature and then for 24 h at 65 °C.

Table 1
The content of metallic impurities in the used processing additives of technical purity.

	Darvan C-N	Duramax B-1014	PEG	Dow Corning B-310
Si [wt.%]	0	0	0	0.77 ± 0.06
Ca [wt.%]	0	0.46 ± 0.01	0.009 ± 0.000	0.38 ± 0.02
Mg [wt.%]	0	0.145 ± 0.003	0.004 ± 0.000	0.119 ± 0.004
Na [wt.%]	0	0.125 ± 0.002	0.041 ± 0.004	0.11 ± 0.02
K [wt.%]	0	0.002 ± 0.000	0	0.016 ± 0.000

Dried tapes were sintered in an electrical furnace with $MoSi_2$ heating elements (CLASIC CZ, Czech Republic) for 4 h at 1600 °C at a heating rate from 2.5 to 10 °C min^{-1}. The heating schedule facilitating safe burn out of organic processing additives was optimized on the basis of data obtained by differential thermal analysis measurements (DTA-Derivatograph Q-1500 D, MOM, GTA). The density of sintered samples was measured by Archimedes method in water. The microstructure of prepared materials was examined by scanning electron microscopy (Zeiss, model EVO 40HV, Carl Zeiss SMT AG, Germany) of polished and thermally etched cross-sections of sintered specimens. The average size of Al_2O_3 matrix grains was estimated by the linear intercept method [25] with the use of the program LINCE (TU Darmstadt, Germany).

The loss tangent was measured as follows [26]. The ceramic plates were coated with the ESL 9912-A silver paste to form a three-electrode system. The diameter of guarded electrode was 20 mm, the separation between the guard and guarded electrode was 1 mm. The low voltage (1 V) measurement of tan δ was performed by the commercial TESLA BM 595 RLCG meter. The maximum available testing frequency was 100 kHz. The measurement at high voltage was carried out at series resonance circuit with three different resonance inductors to set the resonance frequency. The dissipation factor tan δ is defined as the ratio between the real (resistive) and imaginary (capacitive) power delivered to the load. For the dielectric modeled as a resistor and capacitor connected in parallel, the dissipation factor can be expressed as

$$\tan\delta = \frac{I_R}{I_C} \quad (1)$$

where I_C stands for the capacitive current and I_R for the real current. Using this equation, we have placed a low loss HV tunable vacuum capacitor (COMET CVBA; 5–250 pF; 15/9 kV) with the capacity of C_v in parallel to the tested specimen with the capacity of C_x. Electrical current in the circuit was monitored by two calibrated Pearson current monitors Model 2877 fed to the digital oscilloscope LeCroyWaveRunner 6100A. The first of the current monitors was set to sense the electrical current of vacuum capacitor. The second current monitor sensed the difference between the electrical current of vacuum capacitor and the tested specimen. This was accomplished by feeding the corresponding wires through the Pearson monitor's central opening in the opposite direction (see [26] for more details). When the capacity of vacuum capacitor is adjusted to $C_v = C_x$, the first current monitor measures the capacitive current I_C and the second current monitor measures the real current I_R. The actual measurement was carried out at 5 kV of applied voltage. In order to suppress a possible discharge (corona) onset on tested materials, the specimens were immersed in the insulating oil during the procedure.

The microstructure of prepared ceramics was examined on polished and thermally etched (temperature 1450 °C, 2 h isothermal dwell in air) polished cross sections by scanning electron microscope Carl Zeiss EVO 40HV. The phase composition was determined by X-ray powder diffraction analysis with the use of a STOE Automatic X-Ray Powder Diffractometer Systems, Siemens, in the 2θ range from 20° to 75°, CoKα radiation, wavelength 1.7902 Å.

Due to experimental problems encountered during the quantitative chemical analysis of sintered alumina ceramics, the chemical composition and the level of impurities in studied materials was estimated on the basis of chemical analysis of processing organic additives used in tape casting. The concentrations of metallic elements in the organic aids were determined by the optical emission spectroscopy in inductively coupled plasma (Varian Vista MPX), and the results are summarized in Table 1.

3. Results and discussion

The organic processing additives of technical purity used to achieve desired plastic properties of the suspension for tape casting, to ensure sufficient handling strength, and to suppress cracking during drying, contain relatively large amount of metallic impurities (Table 1). The presence of impurities then affects the densification, microstructure and physical properties of final tape. Despite high-applied sintering temperature (1600 °C), all alumina materials prepared by the tape casting method without deliberately added dopants (nominally ''pure'' alumina, later referred to as sample A) contained significant fraction of residual porosity (>4%). The microstructure of the specimen A is shown in Fig. 1. The microstructure is relatively fine-grained, with isometric round-shaped grains with diameters ~1 μm and, despite significant content of impurities like Ca, Si, K, Na, known to trigger abnormal grain growth (AGG), with no obvious signs of AGG. Fig. 2 shows the frequency dependence of loss tangent of the specimen A. It is difficult to assess the influence of individual metallic impurities dissolved in alumina crystal lattice. The chemical composition calculated from the amount of used organic processing additives shows that the contamination is significant. At the first approximation we expect the amounts of Mg^{2+} and Si^{4+} dissolved in the Al_2O_3 crystal lattice to mutually compensate their charges. If Si and Mg are simultaneously present in Al_2O_3 ceramics, their reciprocal solubility is multiplied about 5 times

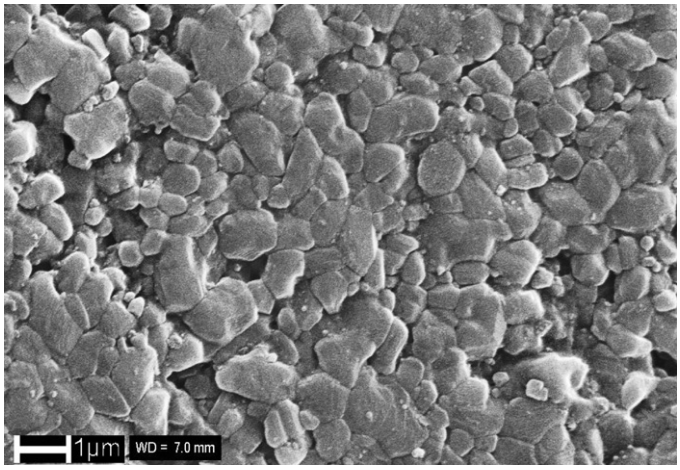

Fig. 1. SEM micrograph of the microstructure of Al_2O_3 ceramics prepared by tape casting without deliberately added dopants and sintered for 4 h at 1600 °C.

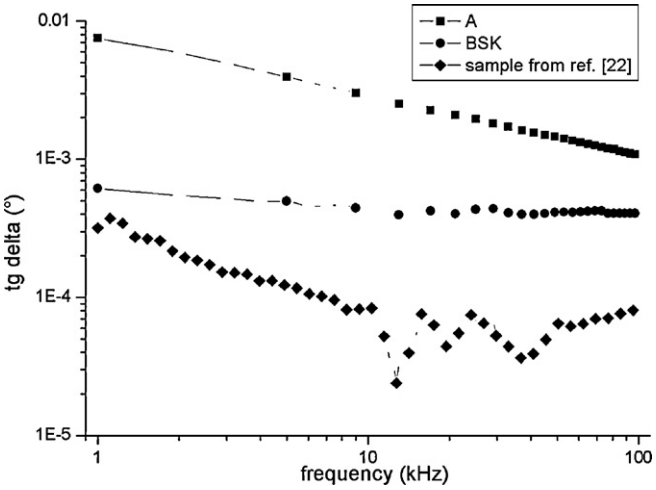

Fig. 2. The frequency dependence on loss tangent for undoped Al_2O_3.

[27,28]. Some Mg segregates at the grain boundaries because the amount of Mg in the material A is 9 times higher than the amount of Si. The redundant Mg then acts against the influence of Ca and suppresses AGG. Excess Mg dissolved in alumina crystal lattice also creates polarizable point defects, which form dipoles in external electric field. A decrease of loss tangent with increasing frequency indicates at least some influence of the dipoles on dielectric losses: at high frequencies the change of polarity of internal dipoles cannot follow the rapidly changing polarity of external electric field and their negative effect on dielectric properties is partly eliminated. However, the loss tangent values two to three orders of magnitude higher than in fully dense materials with carefully controlled chemical composition reported in our previous work (the best sample prepared from suspension with 30 wt.% of Al_2O_3 from reference [22] and commercial sample BSK) indicate that the primary reason for negative action of processing metallic impurities lies in suppression of densification and the presence of residual porosity. The nominally pure alumina prepared by tape casting with the use of organic processing additives of technical purity is thus not suitable as a low loss dielectric material. In the following section the effect of deliberately used additives on microstructure, phase composition, and dielectric properties of alumina ceramics is discussed. Table 2 summarizes the chemical composition (levels of metallic impurities) in all prepared materials, both the deliberately added dopants, and the impurities introduced into the sample by the organic additives of technical purity. The densities and mean grain sizes of respective specimens are also included. Obviously, the levels of impurities introduced by organic processing additives were identical in all specimens, and any significant changes of chemical composition were only achieved by deliberate addition of individual metallic elements.

Considering the complex chemical composition and high levels of impurities in Al_2O_3 ceramics, it is not possible to assess exactly the influence of individual deliberately added dopants on the microstructure development (Fig. 3). The addition of densification supporting and the AGG suppressing dopants (MgO, TiO_2) results in the increase of relative density, and better elimination of residual porosity. With the exception of the addition of MgO, where the presence of Mg suppressed the anisotropic grain growth and resulted in fine-grained microstructure with equiaxial Al_2O_3 grains (Fig. 3a and b), all other specimens contained elongated Al_2O_3 grains as a demonstration of the initial phases of AGG. In some cases, particularly in the sample SAC05 with 0.05 wt.% of CaO the

Table 2
The total contents of metallic impurities, absolute and relative densities and average grain sizes of doped Al_2O_3 materials prepared by tape casting. The amounts of deliberately added dopants are shown in brackets.

	wt.% of elements					Density		Average grain size [µm]
	Mg	Ca	Si	Na	Ti	g cm^{-3}	%	
A	0.11	0.29	0.01	0.10	0	3.786 ± 0.009	95.1 ± 0.2	0.78 ± 0.06
SAM005	0.15 [0.04]	0.29	0.01	0.10	0	3.783 ± 0.005	95.1 ± 0.1	1.7 ± 0.2
SAM05	0.44 [0.33]	0.29	0.01	0.10	0	3.78 ± 0.01	95.1 ± 0.3	2.1 ± 0.2
SAM3	2.07 [1.96]	0.28	0.01	0.10	0	3.856 ± 0.009	97.4 ± 0.2	2.3 ± 0.2
SAC005	0.11	0.33 [0.04]	0.01	0.10	0	3.871 ± 0.006	97.3 ± 0.2	5.8 ± 0.7
SAC05	0.11	0.64 [0.36]	0.01	0.10	0	3.83 ± 0.03	96.3 ± 0.8	–
SAC5	0.10	4.00 [3.70]	0.01	0.09	0	2.996 ± 0.003	75.9 ± 0.1	–
SAT005	0.11	0.29	0.01	0.10	0.03 [0.03]	3.684 ± 0.007	92.6 ± 0.2	1.7 ± 0.2
SAT05	0.11	0.29	0.01	0.10	0.30 [0.30]	3.835 ± 0.001	96.30 ± 0.01	6.9 ± 1.1
SAT5	0.11	0.28	0.01	0.10	2.87 [2.87]	3.821 ± 0.004	95.7 ± 0.1	5.8 ± 0.6

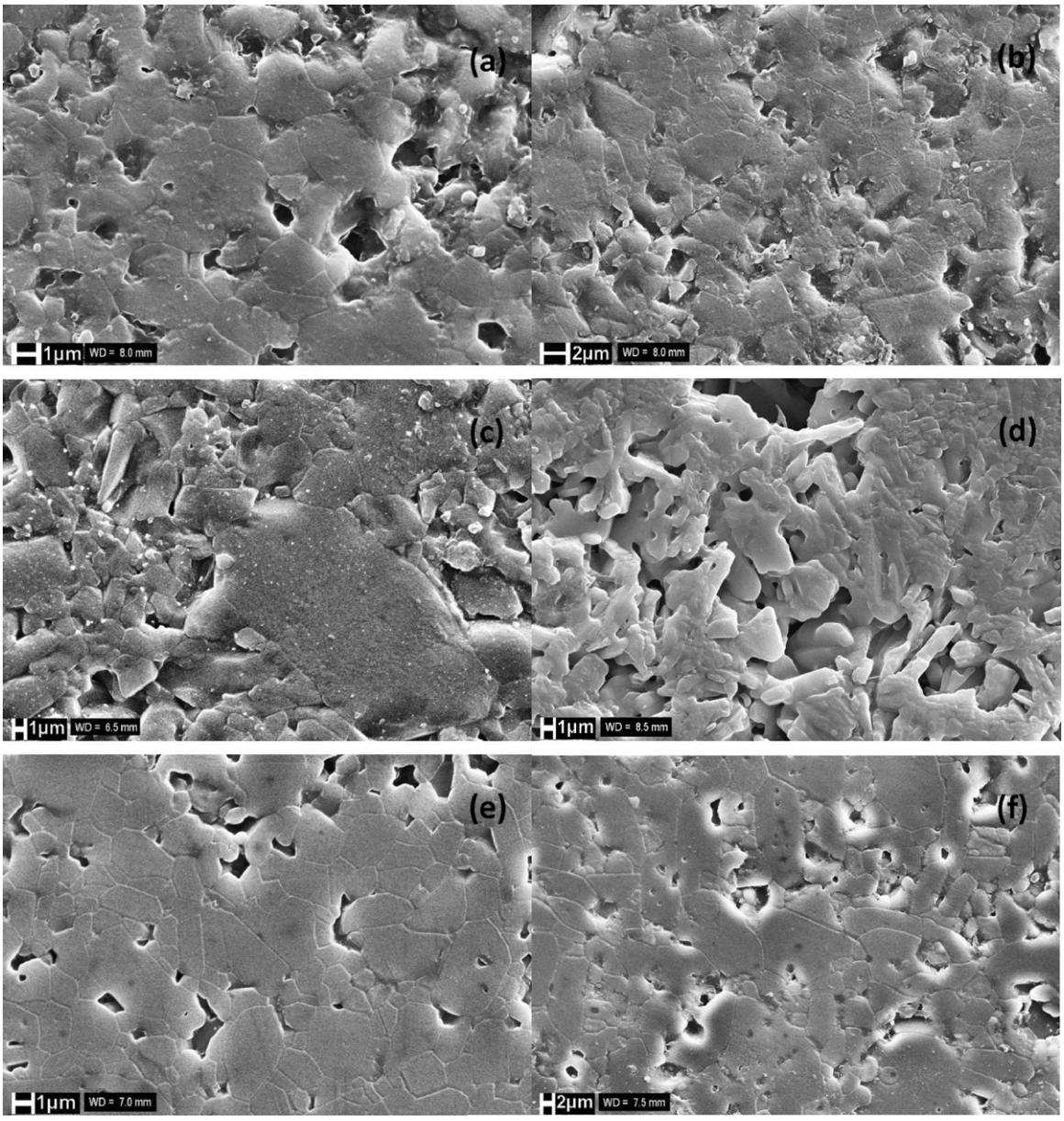

Fig. 3. SEM micrographs of sintered aluminas doped with (a) 0.05 wt.% MgO, (b) 3 wt.% MgO, (c) 0.05 wt.% CaO, (d) 5 wt.% CaO, (e) 0.05 wt.% TiO_2, (f) 5 wt.% TiO_2.

AGG was fully developed and the alumina grains with the size at the level of tens of microns were present in the microstructure.

The values of the average grain size of doped samples are summarized in Table 2. The increase of the content of deliberately added dopants resulted in significant microstructure coarsening in most cases. This is related to the increase of the content of grain boundary melt at the temperature of sintering due to higher overall content of additives in the material. Extreme increase of the mean grain size was observed especially in TiO_2-doped samples (0.5 and 5 wt.% addition) due to the ability of TiO_2 to form a low viscosity melt, which decreased the temperature required to trigger the grain growth. Fig. 4 shows X-ray diffraction patterns of samples doped with 5 wt.% (or 3 wt.% in case of MgO) of additives. Despite of relatively high content of impurities from organic processing additives, no crystalline phases apart from α-Al_2O_3 were detected by X-ray diffraction in specimens with lower levels of deliberately added dopants. These were formed only in highly doped specimens, either by solid state reaction of the dopants with Al_2O_3 matrix or by crystallization from aluminisilicate grain boundary melt. Binary aluminates, namely $MgAl_2O_4$ and Al_2TiO_5, were present in MgO and TiO_2 doped specimens, respectively. Two phases, namely $CaAl_4O_7$ and $CaAl_{12}O_{19}$, were detected in the CaO-doped sample (Fig. 4b).

It is well documented in the literature [29–36] that MgO and TiO_2 positively influence development of microstructure and promote densification. That ability is reflected in the increase of

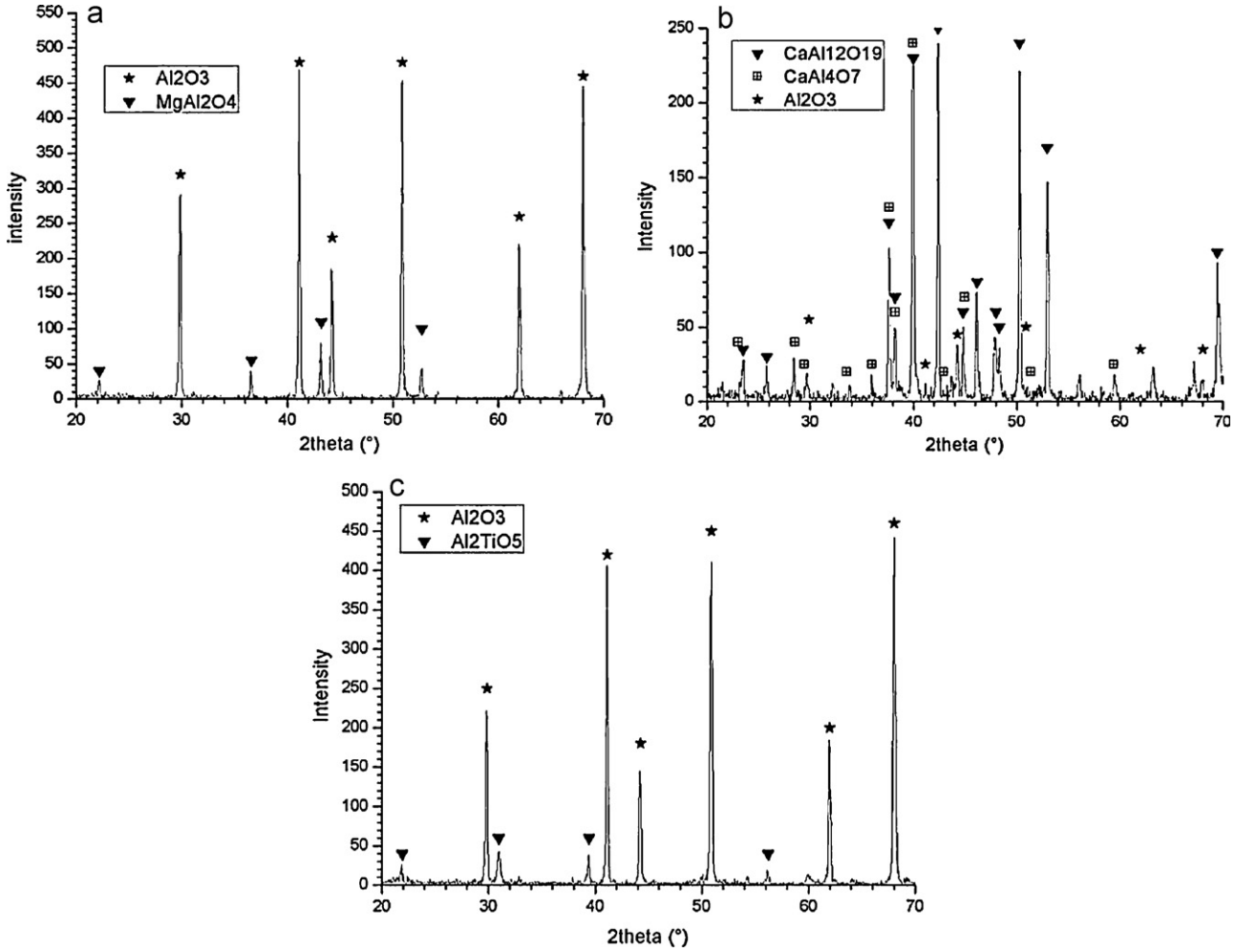

Fig. 4. X-ray diffraction patterns of samples doped with (a) 3 wt.% of MgO, (b) 5 wt.% CaO, and (c) 5 wt.% TiO_2.

relative density, decrease of residual porosity and normal grain growth of MgO and TiO_2-doped samples. TiO_2 decreases the temperature required for densification by forming a low viscosity grain boundary melt. The influence of CaO on microstructure development is negative: although its presence supports the formation of grain boundary melt, and hence densification, the grains tend to grow abnormally [17,37]. Moreover, the formation of various calcium aluminates by crystallization of the grain boundary melt or by solid state reaction between CaO and alumina matrix hinders densification by grain boundary pinning and results in a loose microstructure with extremely high residual porosity, as is clearly shown in the microstructure of the specimen SAC5 (Fig. 3d, Table 2).

Fig. 5 summarizes the frequency dependence of loss tangent of all deliberately doped samples. The influence of dopants on loss tangent can be considered in terms of their effect on microstructure development, presence of vitreous and crystalline secondary phases, and the formation of polarizable point defects in alumina crystal lattice. The presence of oxides with a different valency, which dissolve in the Al_2O_3 structure, causes the formation of polarizable defects and increases the dielectric losses. As mentioned above, the solubility of CaO and MgO ranges depending on the sintering temperature from several tens to hundreds of ppm. TiO_2 is highly soluble in Al_2O_3 [11,15,16], thus creating a significant potential for formation of a high number of point defects and hence high dielectric losses.

In MgO-doped aluminas the addition of 0.05 wt.% of MgO leads to the increase of dielectric losses in the whole frequency range in comparison to undoped alumina (Fig. 5a). On the contrary, enhanced doping then leads to improvement of dielectric properties, at 3 wt% of MgO achieving the loss tangent values three order of magnitudes lower than the undoped alumina. This effect is attributed to: (1) relatively low solubility of Mg^{2+} ions in alumina crystal lattice, which does not significantly influence the dielectric properties, and (2) positive influence of high addition of magnesia on microstucture development (namely the content of residual porosity). Moreover, the excess magnesia in the specimen SAM3 is bound in the form of the spinel phase, which does not impair the loss tangent values. The doping of impure alumina with MgO can be thus used as a suitable way for improving the dielectric properties of the ceramic, and the materials SAM3 can be considered a low loss dielectric.

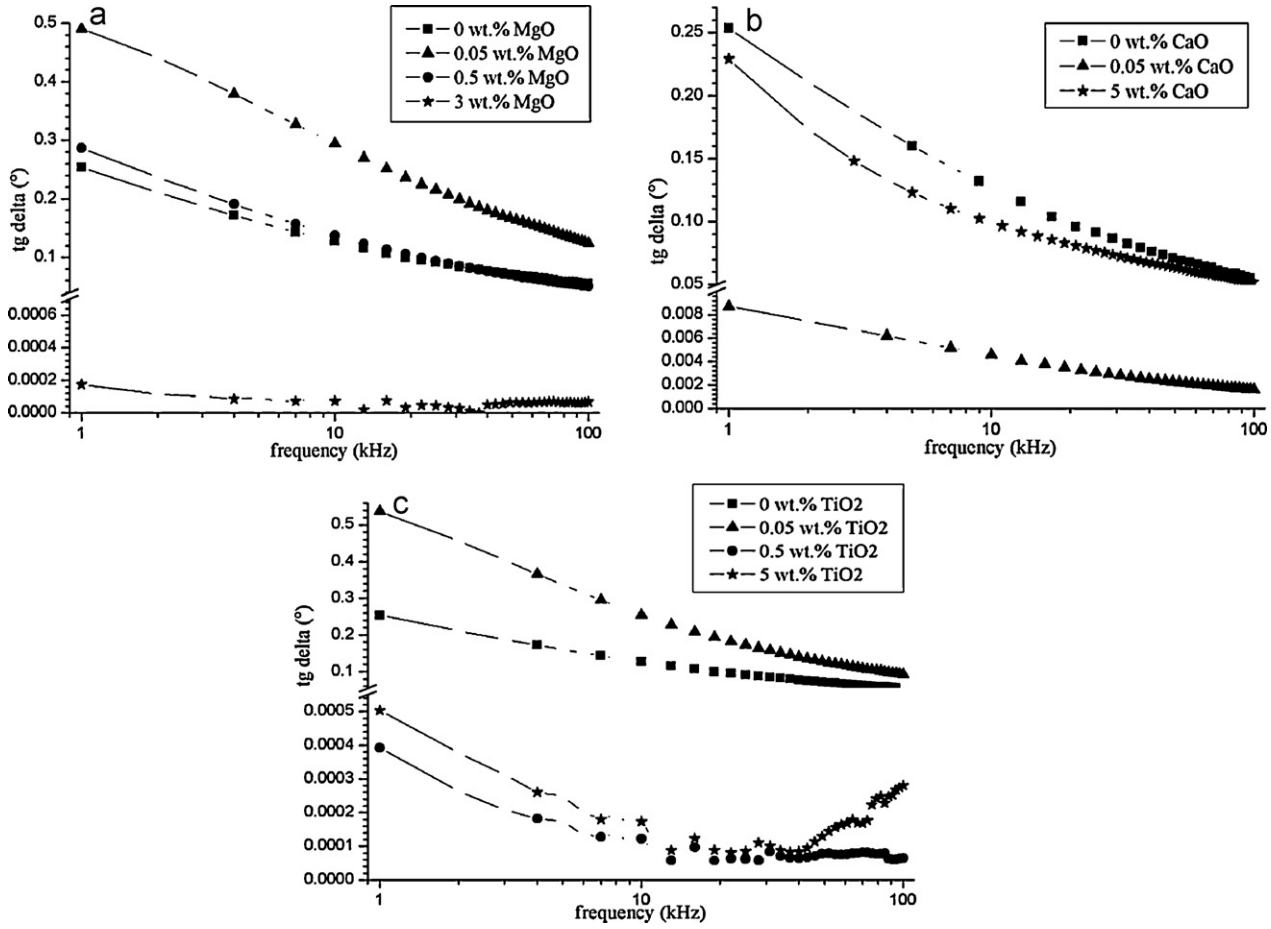

Fig. 5. The frequency dependence of loss tangent of doped Al_2O_3 ceramics with different contents of (a) MgO, (b) CaO, (c) TiO_2.

The addition of 0.05 wt.% CaO (specimen SAC005, Fig. 5b) results in significant decrease of loss tangent values in comparison to undoped alumina (by two orders of magnitude) to the low loss material region. This is related to relatively high value of relative density (97.2%) and to low solubility of Ca in the Al_2O_3 crystal lattice. Further increase of the CaO content (specimen SAC5) results in the increase of the loss tangent values above the level determined for the undoped alumina. The effect is related especially to negative influence of CaO doping on microstructure development, namely extremely high level of residual porosity (24.1%) and the material's phase composition. High level of residual porosity overlaps any influence possibly caused by other effects, such as the presence of vitreous or crystalline calcium aluminate phases. Moreover, taking into account the stoichiometry of identified calcium aluminate phases ($CaAl_4O_7$ and $CaAl_{12}O_{19}$) where one mole of CaO is bound to two, or even six moles of Al_2O_3, respectively, and the results of X-ray diffraction (Fig. 4b) it is obvious that this material can be in fact considered a ceramic consisting of calcium aluminate matrix with high level of residual porosity. These secondary phases have different dielectric properties in comparison with Al_2O_3. The change of value of loss tangent takes place under the influence of these phases, which together with the high content of residual porosity increase the value of tan δ.

The most interesting results were achieved in aluminas doped by TiO_2. Despite the high solubility of Ti^{4+} in the Al_2O_3 crystal lattice, in most cases the TiO_2 doping led to significant decrease of the loss tangent (Fig. 5c). Slight increase of dielectric losses in the specimen SAT005 in comparison to undoped alumina is attributed to increased content of the residual porosity. In the samples with high content of TiO_2 (0.5 and 5 wt.%), the loss tangent values in the whole frequency range are by three orders of magnitude lower than in undoped aluminas, and rank the materials SAT05 and SAT5 well among the low loss dielectrics. The exact mechanism is not clear but can be attributed to several effects. First, due to its ability to form low viscosity melt at relatively low temperatures, the TiO_2 addition improves densification resulting in homogeneous microstructure with relatively low fraction of residual porosity. Second, the grain boundary melt might bond Ti^{4+} preferentially reducing the amount of Ti, which can be dissolved in alumina lattice and at the same time act as a scavenger, which binds other metallic impurities. As shown by the results of X-ray diffraction, significant amount of Ti is also bound in the form of the crystalline Al_2TiO_5, which decreases the amount of Ti^{4+},

which can be effectively dissolved in alumina lattice. Third, the Ti^{4+} ions dissolved in alumina crystal lattice are likely to cross-compensate the effect of dissolved ions with 2+ valency, especially Ca and Mg, thus reducing the negative influence of other impurities on dielectric losses. However, for firm experimental evidence a detailed TEM analysis will be required. In any case, doping of impure alumina with TiO_2 can be considered as an efficient way to improve the dielectric properties of alumina ceramics.

4. Conclusions

The influence of intentionally added dopants on microstructure and dielectric losses of technically impure polycrystalline alumina prepared by aqueous tape casting was examined. Apart from deliberately added dopants, namely MgO, CaO and TiO_2, the studied materials contained also a significant amount of impurities (Na, K, Ca and Si) originating from organic processing aids used for formulation of slurries for the tape casting. The processing impurities in undoped aluminas impaired densification and resulted in high dielectric losses. The dielectric losses expressed in terms of the loss tangent values could be significantly modified by deliberate addition of other dopants. Especially high concentrations 3 wt.% of MgO and 5 wt.% of TiO_2 resulted in the decrease of loss tangent values in the whole studied frequency range by three orders of magnitude in comparison to undoped alumina. The effect is attributed to (1) improved densification and elimination of residual porosity, (2) formation of vitreous grain boundary phase preferentially scavenging the processing impurities, and (3) in case of the TiO_2 addition, charge cross-compensation of lattice point defects resulting from dissolution of the ions with the 2+ valency (Mg, and Ca) in alumina crystal lattice.

Acknowledgments

The financial support of this work by the grant VEGA 2/0076/10, VEGA 2/0178/10, and the APVV grant APVV 0485-06 is gratefully acknowledged. This publication was created in the frame of the project ''Centre of Excellence for Ceramics, Glass, and Silicate materials'' ITMS code 262 201 20056, based on the Operational Program Research and Development funded from the European Regional Development Fund.

The donation of the Al_2O_3 powder CT3000 SG LS by the company Almatis GmbH, Germany is greatly appreciated. The authors wish to express their thanks to Dr. Dagmar Galuskova from the Joint Glass Centre Vitrum Laugaricio for chemical analysis of organic processing additives.

References

[1] M. Šimor, J. Rahel, P. Vojtek, A. Brablec, M. Černák, Atmospheric-pressure diffuse coplanar surface discharge for surface treatments, Appl. Phys. Lett. 81 (2002) 2716–2718.
[2] M. Černák, Int. Patent PCT/SK02/000008 (May 4, 2001).
[3] M. Černák, M. Šimor, J. Ráhel', Electrode element for generating a diffusion co-planar barrier surface electric discharge and production method thereof, SK Patent SK1362003 A3 (November 3, 2004).
[4] S.J. Penn, N.M. Alford, A. Templeton, X. Wang, Effect of porosity and grain size on microwave dielectric properties in sintered alumina, J. Am. Ceram. Soc. 80 (1997) 1885–1888.
[5] J. Molla, R. Heidinger, A. Ibarra, Alumina ceramics for heating systems, J. Nucl. Mater. (1994) 212–215.
[6] M.P. Harmer, R.J. Brook, The effect of MgO additions on the kinetics of hot pressing in Al_2O_3, J. Mater. Sci. 15 (1980) 3017.
[7] S.J. Bennison, M.P. Harmer, Grain-growth kinetics for alumina in the absence of a liquid phase, J. Am. Ceram. Soc. 68 (1985) C22–C24.
[8] R.L. Coble, Sintering and grain growth in alumina and magnesia, in: W.D. Kingery (Ed.), Advances in Ceramics, Vol. 10. Structure and Properties of MgO and Al_2O_3 Ceramics, Am. Ceram. Soc., Columbus, OH, 1984 , p. 839.
[9] N.W. Ashcroft, N.D. Mermin, Solid State Physics, Holt-Saunders, Tokyo, 1976 (Chapter 27).
[10] O.F. Schirmer, Smoky coloration of quartz caused by bound small hole polar on optical absorption, Solid State Commun. 18 (1976) 1349.
[11] S.K. Roy, R. Coble, Solubility of magnesia, titania, and magnesium titanate in aluminium oxide, J. Am. Ceram. Soc. 51 (1968) 1–6.
[12] C. Greskovich, J.A. Brewer, Solubility of magnesia in polycrystalline alumina at high temperatures, J. Am. Ceram. Soc. 84 (2001) 420–425.
[13] K. Ando, M. Momoda, Solubility of MgO in single-crystal Al_2O_3, J. Ceram. Soc. Jpn. 95 (1987) 381–386.
[14] L. Miller, A. Avishai, D.W. Kaplan, Solubility limit of MgO in Al_2O_3 at 1600 °C, J. Am. Ceram. Soc. 89 (2006) 350–353.
[15] E.R. Winkler, J.F. Sarver, I.B. Cutler, Solid solution of titanium dioxide in aluminium oxide, J. Am. Ceram. Soc. 49 (1966) 634–637.
[16] W.D. Mckee, E. Aleshin, Aluminium oxide–titanium oxide solid solution, J. Am. Ceram. Soc. 46 (1963) 54–58.
[17] S.I. Bae, S. Baik, Determination of concentrations of silica and/or calcia for abnormal grain growth in alumina, J. Am. Ceram. Soc. 76 (1993) 1065–1067.
[18] R. Vila, M. González, J. Mollá, A. Ibarra, Dielectric spectroscopy of alumina ceramics over a wide frequency range, J. Nucl. Mater. 253 (1998) 141–148.
[19] J. Mollá, R. Moreno, A. Ibarra, Effect of Mg doping on dielectric properties of alumina, J. Appl. Phys. 80 (1996) 1028–1032.
[20] Ch.J. Wang, Ch.Y. Huang, Effect of TiO_2 addition on the sintering behaviour, hardness and fracture toughness of ultrafine alumina, Mater. Sci. Eng. A492 (2008) 306–310.
[21] A.I.Y. Tok, F.Y.C. Boey, K.A. Khor, Tape casting of high dielectric ceramic composite substrates for microelectronics application, J. Mater. Process. Technol. 8 (1999) 469–472.
[22] J. Chovanec, K. Ghillányová, R. Ráhel', P, Šajgalík, D. Galusek, The influence of dopants on loss tangent of polycrystalline alumina ceramics. Ceram. Int., in press.
[23] N.M. Alford, S.J. Penn, Sintered alumina with low dielectric loss, J. Appl. Phys. 80 (1996) 5895–5898.
[24] N.M. Alford, J. Breeze, X. Wang, S.J. Peen, Dielectric loss of oxide crystal and polycrystalline analogues from 10 to 320 K, J. Eur. Ceram. Soc. 21 (2001) 2605–2611.
[25] J. Ráhel', D.M. Sherman, The transition from a filamentary dielectric barrier discharge to a diffuse barrier discharge in air at atmospheric pressure, J. Phys. D: Appl. Phys. 38 (2005) 547–554.
[26] M.I. Mendelson, Average grain size in polycrystalline ceramics, J. Am. Ceram. Soc. 52 (1969) 443–446.
[27] K.L. Gavrilov, S.J. Benison, K.R. Mikesk, L. Setti, Role of magnesia and silica in alumina microstructure evolution, J. Mater. Sci. 38 (2003) 3965–3975.
[28] K.L. Gavrilov, S.J. Bennison, K.R. Mikeska, J.M. Chabala, R. Levi-Seti, Silica and magnesia dopant distributions in alumina by high-resolution scanning secondary ion mass spectrometry, J. Am. Ceram. Soc. 82 (1999) 1001–1008.
[29] D.S. Kim, et al., Improvement of translucency in Al_2O_3 ceramics by two-step sintering technique, J. Eur. Ceram. Soc. 27 (2007) 3629–3632.

[30] R.L. Coble, Sintering crystalline solids. II. Experimental test of diffusion models in powder compacts, J. Appl. Phys. 32 (1961) 793–799.
[31] J.G.J. Peelen, Sintering and Catalysis, Plenum Press, New York, 1975, pp. 443–453.
[32] M.P. Harmer, E.W. Roberts, R.J. Brook, Rapid sintering of pure and doped Al_2O_3, Trans. Br. Ceram. Soc. 78 (1979) 22–25.
[33] B.K. Kim, S.H. Hong, S.H. Lee, D.Y. Kim, Alternative explanation for the role of magnesia in the sintering of alumina containing small amounts of a liquid phase, J. Am. Ceram. Soc. 86 (2003) 634–639.
[34] A. Kebbede, J. Parai, A.H. Carim, Anisotropic grain growth in α-Al_2O_3 with SiO_2 and TiO_2 additions, J. Am. Ceram. Soc. 83 (2000) 2845–2851.
[35] C.H.L. Huang, J.J. Wang, Ch.Y. Huang, Microwave dielectric properties of sintered alumina using nano-scaled powders of α alumina and TiO_2, J. Am. Ceram. Soc. 90 (2007) 1487–1493.
[36] C.H.J. Wang, Ch.Y. Huang, Effect of TiO_2 addition on the sintering behaviour, hardness and fracture toughness of ultrafine alumina, Mater. Sci. Eng. A492 (2008) 306–310.
[37] J. Jung, S. Baik, Abnormal grain growth of alumina: CaO effect, J. Am. Ceram. Soc. 86 (2003) 644–649.